Supplementary information: Femtosecond Tracking of Carrier Relaxation in Germanium with Extreme Ultraviolet Transient Reflectivity

Supplementary Note S1: Characterization of Pump Pulses by Dispersion Scan.

A dispersion scan [1] was used to characterize the pulse duration of the NIR pump pulse. Briefly, the pump pulse (bottom left, red curve), is frequency doubled using a beta barium borate (BBO) optic, yielding a frequency doubled spectrum (bottom left, blue curve). The doubled frequency is then modified by introducing wedges of known dispersion, yielding a second harmonic spectrum as a function of wedge insertion (top left panel). A reconstruction algorithm then retrieves the phase and electric field of the linear spectrum, indicating a short pulse of 3.7 fs (FWHM).

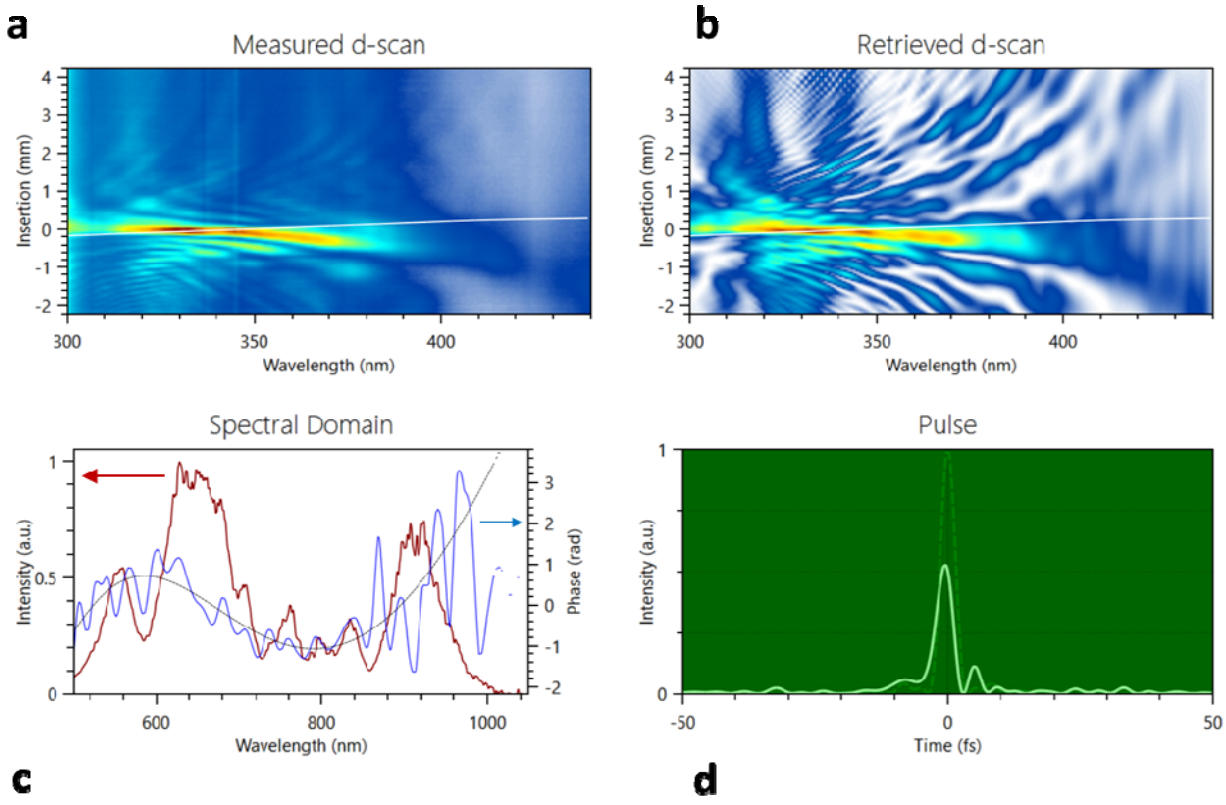

Figure S1: Characterization of pulses using Dispersion Scan. (**a**) Measured second harmonic intensity as a function of wedge insertion. (**b)** Retrieved second harmonic intensity using simulated pulse. **(c)** Pump spectrum (red), phase (blue) and polynomial fit of phase (black line). (**d)** Retrieved pulse intensity has a duration of 3.7 fs FWHM.

Supplementary Note S2: Extreme Ultraviolet Probe spectrum

The Extreme Ultraviolet probe was produced by high harmonic generation in Xe using a flowing gas cell with backing pressure ~24 mTorr. The resulting harmonics span 25-40 eV (**Fig S2**) and have a temporal duration less than or equal to that of the pump pulse, due to the nature of the high harmonic generation process. [2]

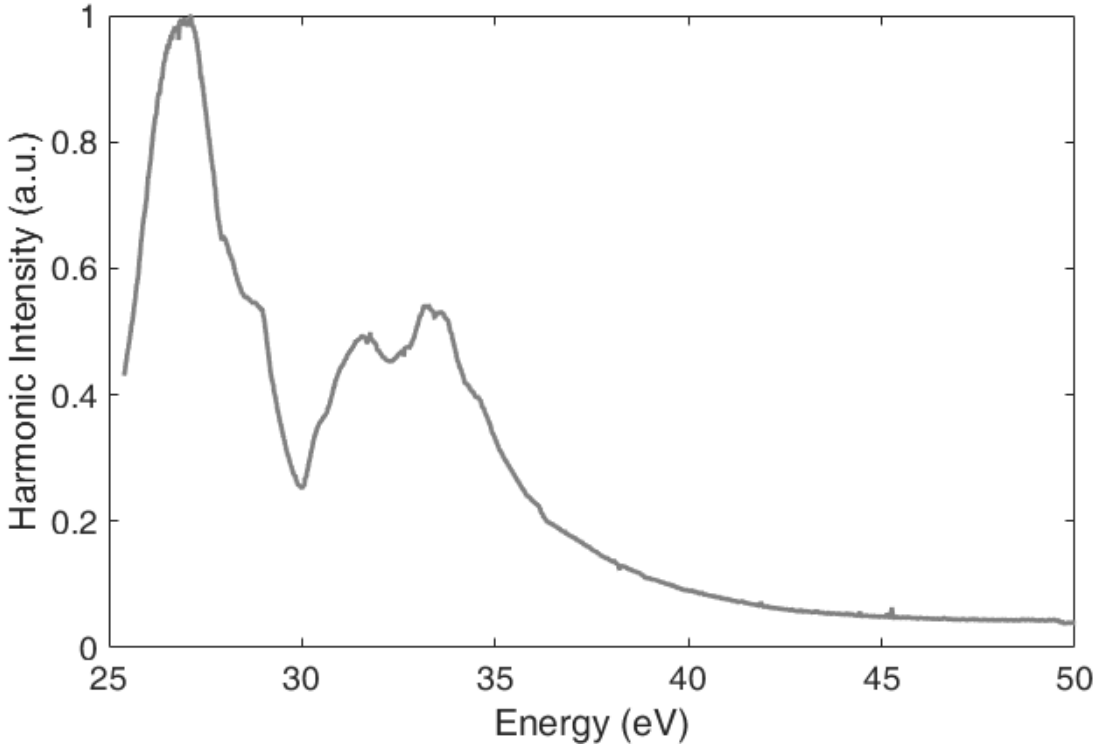

Figure S2: High harmonic spectrum generated in Xenon, reflected on Au mirror, s-polarized.

Supplementary Note S3: Recovery of Static Dielectric function

In order to retrieve the static dielectric function of the germanium sample, 6 multi angle measurements of p-pol reflectivity were performed at the Advanced Light Source and fit to the appropriate Fresnel equation.

$$R_s = \left| \frac{n_1 \cos\theta_i - n_2 \sqrt{1-\left(\frac{n_1}{n_2}\sin\theta_i\right)^2}}{n_1 \cos\theta_i + n_2 \sqrt{1-\left(\frac{n_1}{n_2}\sin\theta_i\right)^2}} \right|^2 \quad \textbf{(S1)}$$

Where R_p is the reflectivity of p-polarized light, $n_2 = \sqrt{\epsilon}$ is the complex-valued index of refraction of the wafer , θ_i is the angle of incidence measured from normal, and n_1 is the index of refraction of the vacuum. Since the pressure in the experimental chamber is ~1x10^{-7} Torr, we take n_1 to be 1. In the fitting procedure, data at θ_i=60, 65, 70, 75, 80, 85° from the surface normal were used. The static reflectivities used in the fit are shown in Figure S3.

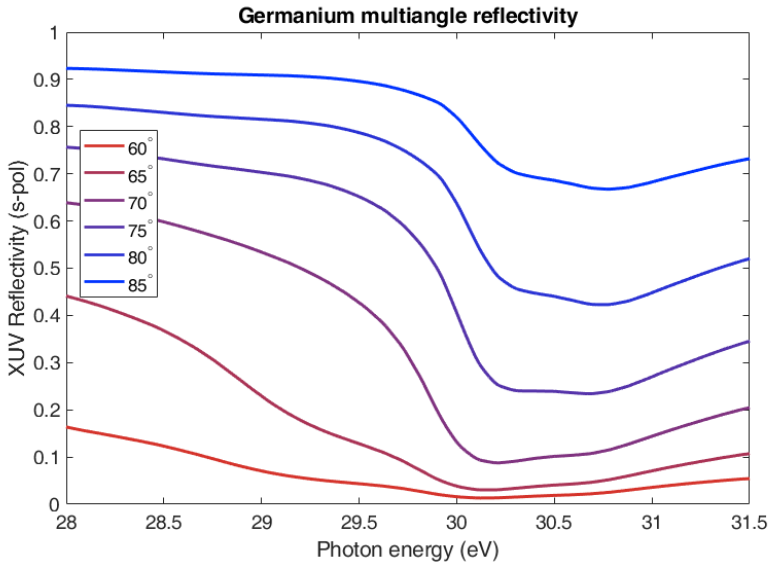

Figure S3: Multi angle reflectivity of germanium, acquired at Advanced light sourced.

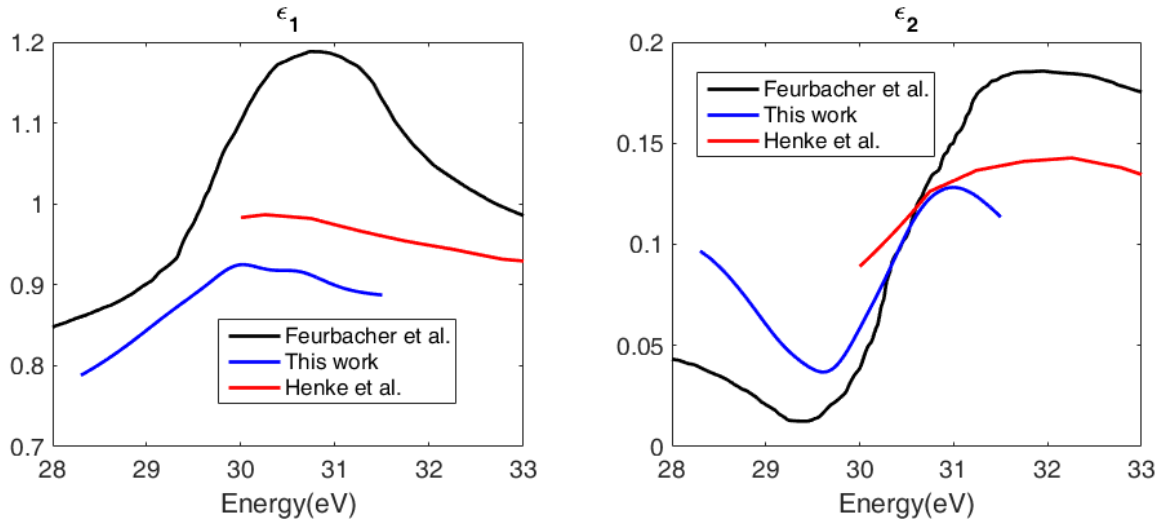

Figure S4: Recovered static dielectric function of germanium. Left (real part), right (imaginary part), both compared to previously published results. [3,4]

Supplementary Note S4: Fitting of Transient Dielectric Function

An iterative fit was employed to retrieve the time-resolved dielectric function from the measured transient reflectivity. In order to separate carrier and shift contributions to the observed transient reflectivity, the observed transient signals were fit via the Fresnel equations to a transient dielectric function of the form:

$$\begin{aligned} \epsilon_{\text{exc}}(\omega) &= \epsilon_{\text{shift}}(\omega) + \epsilon_{\text{carrier}}(\omega) \\ &= \epsilon_{\text{shift}}(\omega) + \epsilon_{\text{holes}}(\omega) + \epsilon_{\text{electrons}}(\omega) \\ \epsilon_{\text{exc}}(\omega) &= \epsilon_0(\omega - \mathrm{E}_{\text{shift}}) + \frac{\omega_{p,h}^2}{\omega_{0,h}^2 - \omega^2 + i\omega\Gamma_h} - \frac{\omega_{p,e}^2}{\omega_{0,e}^2 - \omega^2 + i\omega\Gamma_e} \end{aligned} \qquad \textbf{(S2)}$$

In equation **(S2)**, $\epsilon_0(\omega)$ is the ground state dielectric function (measured by multi angle reflection), and $\omega_{p,h}, \omega_{p,e}, \omega_{0,h}, \omega_{0,e}$, Γ_h, and Γ_e parameterize the amplitude, central frequency, and width of excited electron and hole induced changes in the dielectric function. Similarly, $\epsilon_0(\omega - \mathrm{E}_{\text{shift}})$ describes the impact of global shifts in the excited state dielectric function. For the fit of the experimental data to **S2**, first the shift contribution was fixed, while the carrier contributions were fit using a least squares minimization. The optimal carrier contribution was then averaged with the carrier contribution retrieved from the previous iteration. Subsequently, the carrier contributions were held fixed, and the shift contribution was fit using the same least squares minimization, and similarly averaged with the shift

contribution from the previous iteration. By iterating this procedure until the sum of the residuals changed by $<10^{-12}$, a good agreement between the observed transient reflectivity (Fig 1d), and the reconstructed reflectivity (Fig. 2d) was obtained. Typically, convergence was reached within 5 iterations. This process was repeated for each time point, starting at 10 ps, and working backward, with the output of the finished time point used as the initial guess of the subsequent time point. For the 10 ps time point, an initial guess of the parameters was chosen such that the computed $\Delta R/R$ reasonably represented the data, however the retrieved dielectric function showed little sensitivity to the initial guess used.

Supplementary Note S5: Diffusion Model of Carrier Dynamics

To model the kinetics of the time-resolved dielectric function, the carrier dynamics were compared to a 3 temperature model (3TM) adapted from previous work [5,6] which includes the effects of carrier diffusion, Auger recombination, and the spatial dependence of the carrier distribution.

$$\frac{\partial n_e}{\partial t} = \frac{\partial}{\partial x}\left(D_a \frac{\partial n_e}{\partial x}\right) - \frac{n_e}{\tau_{Aug}(n_e)} + S(x,t) \quad \textbf{(S3)}$$

$$D_a = D_0 T_a^{-1}\sqrt{T_e} \quad \textbf{(S4)}$$

$$C_e \frac{\partial T_e}{\partial t} = \frac{D_a C_e}{n_e}\frac{\partial n_e}{\partial x}\frac{\partial T_e}{\partial x} - \frac{C_e}{\tau_{eo}}(T_e - T_o) - \frac{C_e}{\tau_{ea}}(T_e - T_a) + E_g \frac{n_e}{\tau_{Aug}(n_e)} + \left(\hbar\omega - E_g\right)\cdot S(x,t) \quad \textbf{(S5)}$$

$$C_o \frac{\partial T_o}{\partial t} = \frac{C_e}{\tau_{eo}}(T_e - T_o) - \frac{C_o}{\tau_{oa}}(T_o - T_a) \quad \textbf{(S6)}$$

$$C_a \frac{\partial T_a}{\partial t} = \frac{\partial}{\partial x}\left(C_a D_a \frac{\partial T_e}{\partial x}\right) + \frac{C_e}{\tau_{ea}}(T_e - T_a) + \frac{C_o}{\tau_{oa}}(T_o - T_a) \quad \textbf{(S7)}$$

In equations **S3-S4**, n_e is the excited carrier density, D_a is the temperature dependent ambipolar electronic diffusion coefficient of germanium [7], D_0 is the ambipolar electronic diffusion coefficient at room temperature, [8] T_a and T_o are the temperatures of the acoustic and optical phonon baths, T_e is the excited carrier temperature, τ_{Aug} is the auger recombination rate, [9] and $S(x,t)$ is a source term, (a hyperbolic cosine squared pulse with 5 fs full width at half max, with 800 nm wavelength). In **S5-S7**, C_e, C_o, and C_a refer to the heat capacities of the electronic, optical phonon, and acoustic phonon baths respectively, τ_{eo}, τ_{ea}, and τ_{oa} refer to the electron-phonon, and phonon-phonon coupling times. Additionally, C_a is the thermal diffusion

coefficient of germanium. The heat capacity of the acoustic phonons is modeled using an Debye model with a Debye temperature of 374 K. [10]

References

[1] F. Silva, M. Miranda, B. Alonso, J. Rauschenberger, V. Pervak, and H. Crespo, Opt. Express **22**, 10181 (2014).

[2] F. Krausz and M. Ivanov, Rev. Mod. Phys. **81**, 163 (2009).

[3] B. Feurbacher, M. Skibowski, R. P. Godwin, and T. Sasaki, **58**, 1434 (1969).

[4] B. L. Henke, E. M. Gullikson, and J. C. Davis, Nucl. Data Table **54**, 181 (1993).

[5] S. K. Cushing, M. Zürch, P. M. Kraus, L. M. Carneiro, A. Lee, H.-T. Chang, C. J. Kaplan, and S. R. Leone, arXiv:1705.04393 [Cond-Mat, Physics:physics] 1 (2017).

[6] T. Shin, S. W. Teitelbaum, J. Wolfson, M. Kandyla, and K. A. Nelson, J. Chem. Phys. **143**, 194705 (2015).

[7] S. Zollner, K. D. Myers, K. G. Jensen, J. M. Dolan, D. W. Bailey, and C. J. Stanton, Solid State Commun. **104**, 51 (1997).

[8] J. F. Young and H. M. Van Driel, Phys. Rev. B **26**, 2147 (1982).

[9] E. Gaubas and J. Vanhellemont, J. Electrochem. Soc. **154**, H231 (2007).

[10] C. A. and E. of the L. V. III/17A-22A-41A1b, in *Gr. IV Elem. IV-IV III-V Compd. Part B - Electron. Transp. Opt. Other Prop.* (Springer-Verlag, Berlin/Heidelberg, n.d.), pp. 1–7.